PACS numbers: 42.65.Jx; 42.65.Ky; 42.65.Re
DOI: 10.1070/QE2015v045n05ABEH015766

Self-phase modulation in a thin fused silica plate upon interaction with a converging beam of down-chirped femtosecond radiation

Ya.V. Grudtsyn, I.G. Zubarev, A.V. Koribut, I.E. Kuchik, S.B. Mamaev, L.D. Mikheev, S.L. Semjonov, S.G. Stepanov, V.A. Trofimov, V.I. Yalovoi

Abstract. **The mechanism of spectral broadening and self-compression of down-chirped femtosecond pulses in the visible range (473 nm) upon nonlinear interaction of a converging Gaussian beam with a 1-mm-thick fused silica plate is experimentally and theoretically investigated. It is found experimentally that when the intensity increases and plasma is formed in the sample, the regime of femtosecond pulse splitting is transformed into the single-pulse generation regime during nonlinear interaction. As a result of self-compression, the duration of the initial transform-limited pulse is reduced by a factor of 3. Based on the numerical solution of the generalised nonlinear Schrödinger equation, with the plasma formation disregarded, it is shown that the profile, spectrum and temporal phase of the pulse transmitted through the sample acquire a stationary shape behind the focal plane of the focusing mirror. The calculation results are in good agreement with experimental data. The possibility of parametric amplification of the pulse spectral components under given experimental conditions is discussed.**

Keywords: *down-chirped femtosecond pulse, self-compression, self-phase modulation, four-wave mixing.*

1. Introduction

In this paper, we report the results of studying the mechanism of spectral broadening and self-compression of down-chirped femtosecond pulses in the visible range (473 nm) under nonlinear interaction of converging beams with fused silica. This phenomenon was observed for the first time in [1] using diverging femtosecond beams. Our study is aimed at developing new, relatively simple methods of self-compression of femtosecond pulses, which would expand experimental possibilities of their shortening and could be applied to higher energy pulses. The known self-compression methods based on beam filamentation in gases and solids (see, e.g., [2–5]) and ionisation self-compression in gas-filled capillaries (see, e.g., [6, 7]) have limitations on the pulse energy (several millijoules and several tens of millijoules, respectively).

Ya.V. Grudtsyn, S.B. Mamaev, S.G. Stepanov, V.I. Yalovoi P.N. Lebedev Physics Institute, Russian Academy of Sciences, Leninsky prosp. 53, 119991 Moscow, Russia;
I.G. Zubarev, L.D. Mikheev P.N. Lebedev Physics Institute, Russian Academy of Sciences, Leninsky prosp. 53, 119991 Moscow, Russia; National Research Nuclear University 'MEPhI', Kashirskoe sh. 31, 115409 Moscow, Russia;
e-mail: zubarev@sci.lebedev.ru, mikheev@sci.lebedev.ru;
A.V. Koribut Moscow Institute of Physics and Technology (State University), Institutskii per. 9, 141707 Dolgoprudnyi, Moscow region, Russia;
I.E. Kuchik, V.A. Trofimov M.V. Lomonosov Moscow State University, Vorob'evy gory, 119991 Moscow, Russia;
S.L. Semjonov Fiber Optics Research Center, Russian Academy of Sciences, ul. Vavilova 38, 119333 Moscow, Russia; e-mail: sls@fo.gpi.ru

Received 29 January 2015; revision received 12 February 2015
Kvantovaya Elektronika **45** (5) 415–420 (2015)
Translated by Yu.P. Sin'kov

2. Experimental

Figure 1 shows the optical scheme of our experiments. Initial transform-limited 70-fs pulses with a wavelength of 473 nm were generated by doubling the frequency of a laser beam generated by a Ti:sapphire laser system (Avesta-Project Ltd.). A negative quadratic phase was introduced into the beam using a prism pair, and the beam was subjected to spatial filtering. As a result, down-chirped pulses with a duration of ~130 fs, energy up to 0.6 mJ and spectral width of ~3 nm, which corresponds to transform-limited 80-fs pulses (in the approximation of a pulse profile described by the function sech^2) were formed. This pulsed radiation was focused on a 1-mm-thick fused silica (KU-I grade) sample, which played the role of the input window of a 45-cm-long vacuum cell. The focal plane of the focusing mirror was behind the sample (inside the vacuum chamber). The incident beam intensity was varied by displacing the sample along laser beam path;

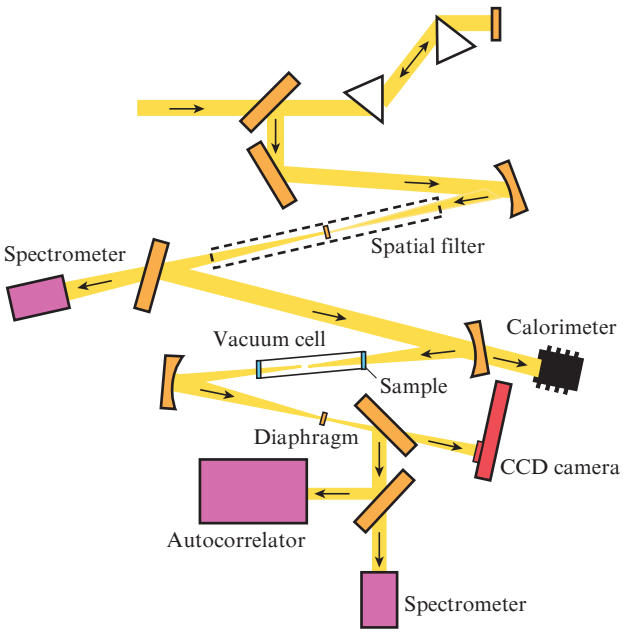

Figure 1. Optical scheme of experiments.

the diameter of the spot on the sample (at a level of $1/e^2$) was varied from 0.15 to 0.27 mm, which made it possible to obtain intensities up to 20 TW cm^{-2}. Enlarged images of different beam cross sections inside the vacuum cell were projected onto a diaphragm 1 mm in diameter using another spherical mirror. We measured the spectrum, profile and energy of the beam incident on the sample; the beam profile and spectrum at different distances from the beam axis at the output of the vacuum cell; and the spatial profile, spectrum and autocorrelation function of the radiation transmitted through the diaphragm, the position of which was chosen so as to reduce the pulse duration to minimum.

3. Results

Due to the spatial filtering, the beam incident on the sample was close to Gaussian. The emission spectrum is presented in Fig. 2. Figure 3 shows the beam profile in the diaphragm plane; it looks like a relatively homogeneous core surrounded by diffraction rings. This pattern is due to the addition of a radius-dependent nonlinear phase to the initial spatial phase of a spherically converging wave [8, 9]. Note that the spectral broadening and pulse self-compression were observed only in the beam core. The emission spectrum in a diffraction ring barely differed from the spectrum of the initial beam incident on the sample. The diaphragm cut out the central part of the beam, enclosed in the white ring in Fig. 3. The beam profile in the near-field zone after the diaphragm is shown in Fig. 4.

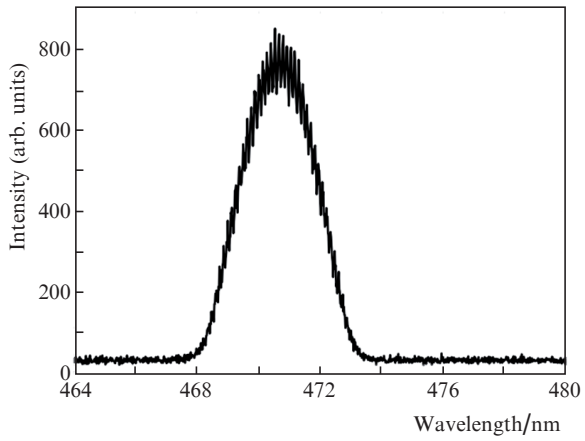

Figure 2. Spectrum of the laser beam incident on the sample.

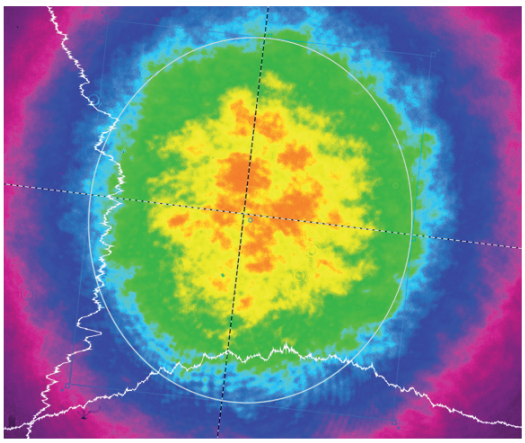

Figure 4. Profile of a beam transmitted through a diaphragm, in the near-field zone.

Figure 5 shows the spectra and autocorrelation functions measured behind the diaphragm at different beam intensities. The significant spectral broadening was observed in the sample at intensities exceeding 3–4 TW cm^{-2}. At intensities below 5–6 TW cm^{-2} almost symmetric spectral broadening with respect to the centre wavelength and splitting of the femtosecond pulse (Fig. 5a) are observed. With an increase in intensity, the spectrum becomes blue-shifted, and the pulse splitting disappears (Figs 5b, 5c); these effects are caused by the plasma formation in fused silica at high beam intensities. The minimum single-pulse duration observed during plasma formation was smaller than the initial duration of the transform-limited pulse by a factor of 3 (Fig. 5c).

The fact of the plasma formation at high beam intensities is confirmed by the presence of significant absorption in the sample (Fig. 6); taking into account that the fused silica band gap is 9 eV and the photon energy is 2.6 eV, the absorption mechanism represents a four-photon process [10, 11].

The self-compression efficiency, defined as the ratio of the pulse energy behind the diaphragm to the energy incident on the sample, is 10%–15%.

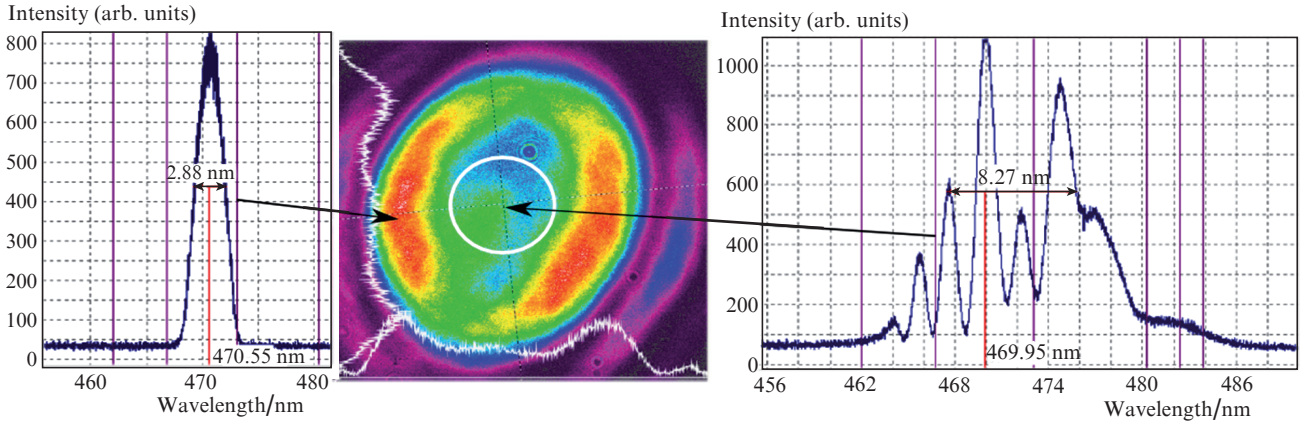

Figure 3. Beam profile in the diaphragm plane and the emission spectra in a diffraction ring and in the beam centre at a beam intensity of 5 TW cm^{-2}.

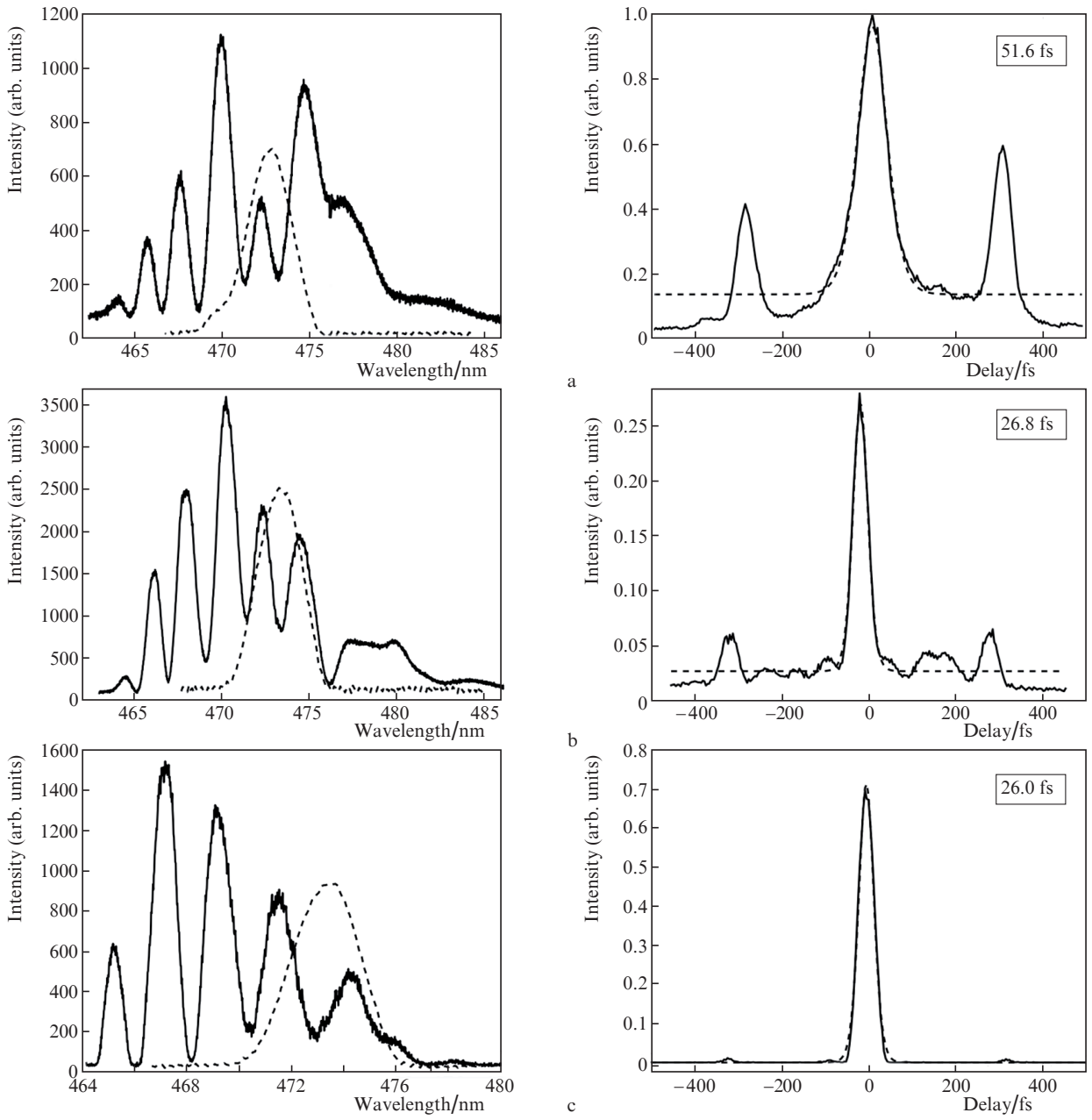

Figure 5. Broadened (solid lines) and initial (dashed lines) spectra (on the left) and autocorrelation functions (on the right), obtained with the aid of an autocorrelator, at intensities of (a) 5, (b) 10 and (c) 15 TW cm^{-2}.

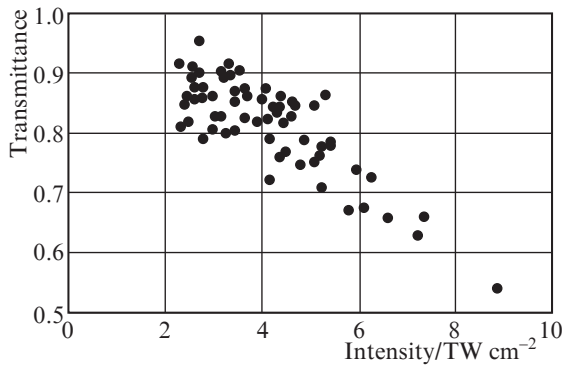

Figure 6. Dependence of the absorption in a 1-mm-thick fused silica sample on the radiation intensity.

4. Discussion

4.1. Numerical simulation using nonlinear Schrödinger equation

The nonlinear interaction of femtosecond radiation with fused silica was modelled based on numerical solution of the three-dimensional generalised nonlinear Schrödinger equation

$$\frac{\partial A(r,t)}{\partial z'} = \left[\frac{\mathrm{i}}{2k_0}\nabla_\perp^2 - \frac{\mathrm{i}}{2}k_2\frac{\partial^2}{\partial t^2} + \frac{\mathrm{i}2\pi n_2}{\lambda}\left(1 + \frac{\mathrm{i}}{\omega_0}\frac{\partial}{\partial t}\right)\right.$$

$$\left.\times\int_0^\infty R(t')I(r,t-t')\,\mathrm{d}t'\right]A(r,t).$$

Here, the first term on the right-hand side describes diffraction, the second term accounts for second-order dispersion and the third takes into account the nonlinearity of the medium and self-steepening. The nonlinear response function $R(t)$ takes into account both the fast (electronic) and slow (molecular) components:

$$R(t) = (1 - f_R)\delta(t) + f_R h_R(t),$$

where the molecular component is described by the function

$$h_R(t) = \frac{\tau_1^2 + \tau_2^2}{\tau_1 \tau_2^2} \exp\left(-\frac{t}{\tau_2}\right) \sin\frac{t}{\tau_1}$$

at $\tau_1 = 12.2$ fs and $\tau_2 = 32$ fs [12]. The contribution of this component to nonlinearity is $f_R = 0.18$ [13, 14].

Calculations were performed for a converging Gaussian beam:

$$A(r, z = 0, t) = \sqrt{I_{max}} \exp\left(-\frac{r^2}{4\rho^2}\right) \exp\left(-ik\frac{r^2}{2R}\right) \times \exp\left[-\frac{2\ln 2(1 + iC)t^2}{T_{1/2}^2}\right],$$

where $R = 4.5$ cm, $\rho = 65$ μm, $T_{1/2} = 123$ fs, $C = -1.2$ (down chirp) and $I_{max} = 4$ TW cm^{-2}. The calculation procedure was separated into two stages: (i) interaction of a converging down-chirped beam with fused silica and (ii) free propagation in space. The group-velocity dispersion for fused silica is $k_2 = 80$ fs^2 mm^{-1} and the nonlinear refractive index is $n_2 = 2.5 \times 10^{-16}$ cm^2 W^{-1} [15].

The calculation results are shown in Fig. 7. One can see that the spectrum, profile and temporal phase of the pulse acquire stationary shapes at a distance of about 10 cm from the sample, i.e., behind the focal plane of the focusing mirror.

Figure 8 shows a numerically calculated spectrum on the beam axis at a distance of 20 cm from the sample and an experimental spectrum behind the diaphragm for a beam

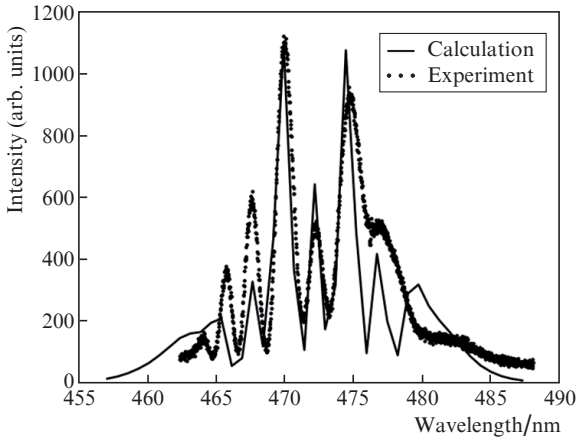

Figure 8. Comparison of the calculated and experimental spectra of radiation behind the sample.

intensity of 5 TW cm^{-2}. The good agreement between the theory and experiment indicates that the main mechanism of spectrum formation at this intensity is self-phase modulation. The calculation demonstrates pulse splitting, which was also observed in experiments.

The pulse splitting in the paraxial region at relatively low beam intensities, when the plasma influence is insignificant, is due to the spatial redistribution of the radiation intensity, at which the radiation near the maximum of the temporal pulse profile, minimally subjected to self-phase modulation, undergoes strong refraction due to the formation of a Kerr lens and is displaced to the beam periphery behind the focal plane of the focusing lens. This radiation does not fall in the diaphragm (cutting out the central part of the beam, which contains radiation corresponding to the leading and trailing edges of the pulse) and, therefore, undergoes the strongest self-phase modulation. In the absence of plasma, the nonlinearity, being basically of electronic type, determines the self-action of the pulse, which is relatively symmetric with respect

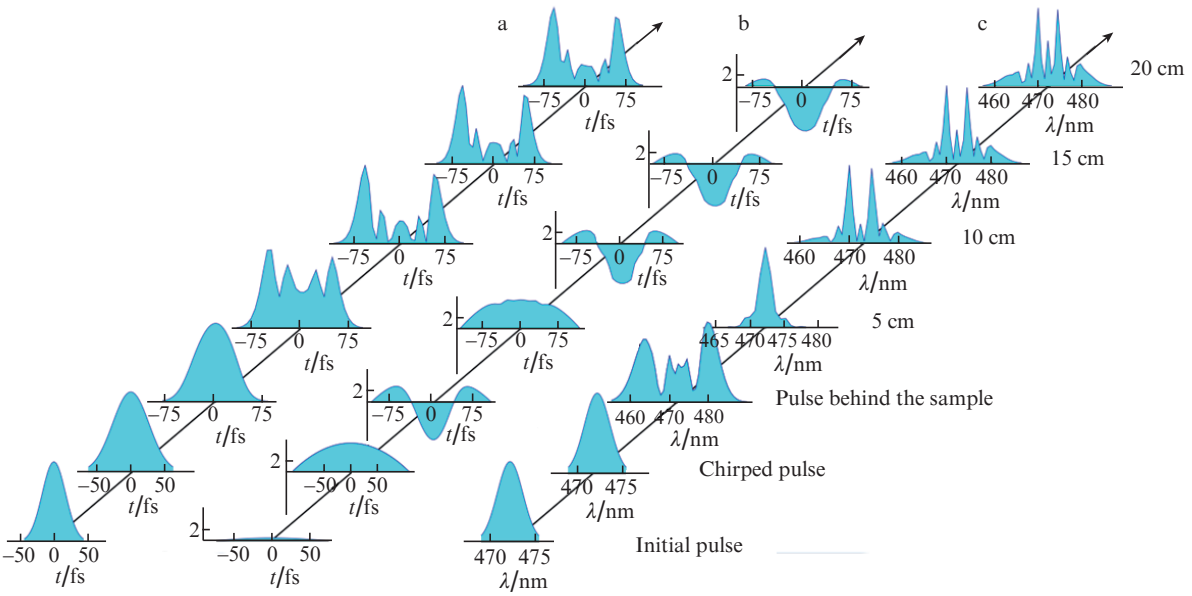

Figure 7. Results of numerical simulation: (a) shape, (b) temporal phase and (c) spectrum of a pulse as functions of the distance from the sample.

to its maximum, in view of which one would expect pulse splitting into two pulses with comparable amplitudes. This conclusion is confirmed by the spectral measurements at the centre of the beam and at its periphery (see Fig. 3), which demonstrate the presence of an unshifted spectral component mainly at the beam periphery.

The formation of plasma leads, on the one hand, to a negative additive to the refractive index and, on the other hand, to asymmetric (with respect to the pulse maximum) self-action because of the long (~150 fs [16]) electron pasma lifetime, which results in selection of one pulse. A more detailed study of the behaviour of the pulse spectrum and pulse shape at radiation intensities higher than 10 TW cm^{-2} calls for numerical consideration of the plasma formation.

4.2. Four-wave mixing

When considering the nonlinear interaction of femtosecond radiation with fused silica, one cannot exclude the influence of four-wave mixing on the formation of spectral and temporal characteristics of radiation in the case where isolated spectral components arise. To determine the fundamental possibility of this influence, we solved numerically the equations for the degenerate case:

$$\frac{dA_p}{dz} = i\gamma_p |A_p|^2 A_p + 2i\gamma_p(|A_s|^2 + |A_i|^2)A_p + 2i\gamma_p A_s A_i A_p^* \exp(i\Delta\beta z),$$

$$\frac{dA_s}{dz} = i\gamma_s |A_s|^2 A_s + 2i\gamma_s(|A_p|^2 + |A_i|^2)A_s + 2i\gamma_s A_p^2 A_i^* \exp(-i\Delta\beta z),$$

$$\frac{dA_i}{dz} = i\gamma_i |A_i|^2 A_i + 2i\gamma_i(|A_p|^2 + |A_s|^2)A_i + 2i\gamma_i A_p^2 A_s^* \exp(-i\Delta\beta z),$$

where $\Delta\beta = k_s + k_i - 2k_p$; A_p, A_s, A_i and k_p, k_s and k_i are, respectively, the complex amplitudes normalised to $(|A_{p0}|^2)^{1/2}$ and wave vectors of the pump, signal and idler waves; z is the longitudinal coordinate, normalised to the sample thickness $L = 0.2$ cm; and $\gamma_s \approx \gamma_i \approx \gamma_p = \omega_p n_2 L|A_{p0}|^2/c$ is the nonlinearity parameter.

In contrast to the widespread slowly-varying-envelope approximation, which is valid only in the initial stage of wave mixing and neglects the influence of the generated wave on the pump amplitude, the approach used by us takes into account the mutual influence of waves and the conservation laws (invariants of wave propagation) for the interaction under consideration. To this end, we used the method proposed in [17] to solve nonlinear equations describing different processes of laser frequency conversion (generation of the second and third harmonics as well as sum and difference frequencies). This method was applied to analyse the regimes of second-harmonic generation with a nonzero initial amplitude [18], for frequency doubling in photonic structures [19], and in some other cases. The conclusions drawn based on this analysis were confirmed by the results of computer simulation on the basis of the numerical solution of the corresponding systems of nonlinear Schrödinger equations.

The essence of this method is to derive an algebraic equation for the phase difference of interacting waves from the system of initial differential equations. To this end, the Hamiltonian (invariant) of the equations under consideration is applied instead of the generally used differential equation with respect to the phase difference of the interacting waves. In this case, the system of equations describing the wave interaction consists of equations with respect to the real amplitudes, equal to square roots of their intensities, and an algebraic equation with respect to the phase difference (instead of the differential equation containing interacting-wave intensities in the right-hand side). Using the ratio between the interacting-wave intensities, which follows from the Manley–Rowe relations, one can derive an equation with respect to the intensity of any wave and integrate it.

This equation contains a fourth-order polynomial with respect to the analysed-wave intensity. Therefore, at certain relations between the polynomial coefficients, which depend on the input-wave intensity, the phase difference of the interacting waves (in the case of nonzero input intensities of all interacting waves) and the mismatch of wave numbers, there are four real roots at which this polynomial turns to zero. Then the intensity of the chosen wave will change within a certain pair of roots, corresponding to the maximum and minimum wave intensities; i.e., the bistable regime of wave interaction will be implemented. The evolution of the change in intensity is described by elliptic functions.

It should be noted that multiplicity of solutions often occurs, i.e., there may be two solutions for the same dimensionless parameters, which correspond to bistable wave interaction. Switching from one interaction regime to the other depends on the parameters of the problem. For example, at some values of interacting-wave amplitudes (and other parameters of the problem), these two solutions have similar values in some cross sections of the medium: the maximum intensity for the lower branch of the solution is close to the minimum intensity for the upper branch of the solution. In this case, the switching is due to the influence of noise. There is a similar bistable regime in the case of second-harmonic generation under conditions of cubic nonlinearity [17, 18]. Its essence is in the fact that, when the input intensity of the pump wave is exceeded (and some other conditions are fulfilled), there may be two (low- and high-efficiency) regimes of second-harmonic generation. The solution obtained is determined by the initial signal-wave intensity and the phase difference of the interacting waves at the input of the medium.

Figure 9 shows examples of solutions for the signal wave gain $R = \max(|a_s(z)|^2/a_{s0}^2)$ under four-wave mixing, depending on the relation between the initial phases, $\varphi_0 = \varphi_{s0} + \varphi_{i0} - 2\varphi_{p0}$, at $\gamma_s = \gamma = 4.7-5.7$, $a_{s0} = a_{i0} = \sqrt{0.2}\, a_{p0}$ and $\Delta\beta = 0.12$ for two branches. Here, a_{j0} and φ_{j0} (j = s, i, p) are the initial values (z = 0) of the real amplitudes and phases of interacting waves in the representation $A_{j0} = a_{j0}\exp(i\varphi_{j0})$.

The results obtained show that there is a fundamental possibility of significant parametric amplification of side spectral components along the direction of femtosecond pulse propagation in a wide range of initial phases. This circumstance may lead to redistribution of band intensities in the beam spectrum without any changes in its structure, which is formed due to the self-phase modulation. Generation of new frequencies and occurrence of additional spectral components due to amplification of spontaneous noise are excluded, because phase-matching conditions are violated for signal and idler waves of low intensities [20]. However, as the calcu-

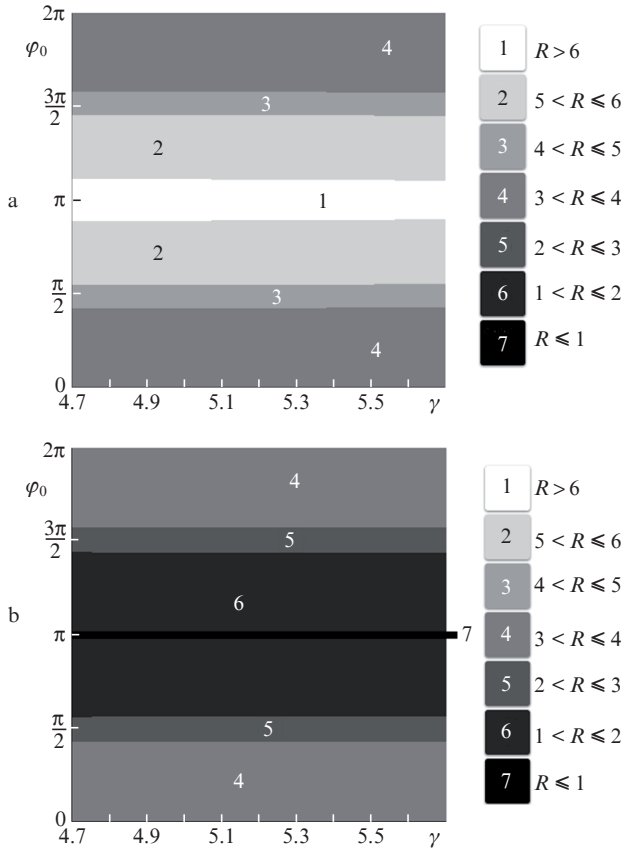

Figure 9. Signal-wave gain R as a function of the initial value of the relative phase φ_0 of interacting waves at $\gamma_s = \gamma = 4.7-5.7$ for the (a) first and (b) second branches.

lations show, at sufficiently high initial intensities of these waves, the self- and cross-phase modulation caused by them leads to phase matching and parametric amplification.

5. Conclusions

Our experimental and theoretical study of the nonlinear interaction of down-chirped femtosecond pulses of visible light (473 nm) with fused silica in converging Gaussian beams revealed the following.

(i) The spectrum undergoes a significant broadening in the sample at intensities exceeding 3–4 TW cm^{-2}; this broadening is inhomogeneous over the cross section of the beam transmitted through the sample and reaches a maximum in its central part, where pulse self-compression is also observed.

(ii) Stationary intensity, phase and spectrum profiles are formed in the paraxial region of the beam behind the focal plane of the spherical mirror focusing the beam onto the sample.

(iii) As in the methods based on filamentation-induced self-compression and self-compression in gas-filled capillaries, plasma (the formation of which is confirmed by the presence of multiphoton absorption in the sample) plays an important role in the generation of single pulses.

Laser beam filamentation does not occur in the self-compression method implemented in this study. The main hindrances are the small sample thickness and high initial intensity of the incident beam, which leads (via multiphoton ionisation) to generation of plasma, and the latter impedes self-focusing. Under these conditions, we reduced the pulse duration by a factor of 3: from 80 fs (the initial duration of spectrally limited pulse) to 26 fs.

It was theoretically shown that four-wave mixing may affect the relative distribution of band intensities in the stage of formation of the spectrum band structure due to the self-phase modulation upon nonlinear interaction of down-chirped femtosecond pulses with fused silica.

The regime of wide-aperture nonlinear interaction calls for a more detailed theoretical and experimental study in order to optimise the self-compression conditions for femtosecond pulses and obtain maximum energy efficiency of the method under consideration and minimum (close to limiting) pulse duration.

Acknowledgements. We are grateful to V.I. Kovalev for the helpful discussions and T.Yu. Moskalev for his help. This work was supported by the Programmes of the Presidium of the Russian Academy of Sciences 'Extreme Light Fields and Their Applications' (Project 1.3) and 'Fundamental Problems of Pulsed High-Current Electronics' and by the Russian Foundation for Basic Research (Grant No. 13-02-01171a).

References

1. Aristov A.I. et al. *Kvantovaya Elektron.*, **42**, 1097 (2012) [*Quantum Electron.*, **42**, 1097 (2012)].
2. Varela O. et al. *Opt. Lett.*, **35**, 3649 (2010).
3. Kurilova M.V. et al. *Kvantovaya Elektron.*, **39**, 879 (2009) [*Quantum Electron.*, **39**, 879 (2009)].
4. Chen X. et al. *Opt. Commun.*, **259**, 331 (2006).
5. Blonskyi I.V. et al. *Ukr. J. Phys. Opt.*, **14**, 85 (2013).
6. Skobelev S.A. et al. *Pis'ma Zh. Eksp. Teor. Fiz.*, **89**, 641 (2009).
7. Skobelev S.A. et al. *Phys. Rev. Lett.*, **108**, 123904 (2012).
8. Nascimento C.M. et al. *J. Opt. A: Pure Appl. Opt.*, **8**, 947 (2006).
9. Villafranca A.B. et al. *J. Opt. A: Pure Appl. Opt.*, **11**,125202 (2009).
10. Stuart B.C. et al. *Phys. Rev. Lett.*, **74**, 2248 (1995).
11. Stuart B.C. et al. *Phys. Rev. B*, **53**, 1749 (1996).
12. Blow K. J., Wood D. *IEEE J. Quantum Electron.*, **25**, 2665 (1989).
13. Stolen R.H. *J. Opt. Soc. Am. B*, **6**, 1159 (1989).
14. Agrawal G.P. *J. Opt. Soc. Am. B*, **28**, A1 (2011).
15. Artiglia M. *Opt. Fiber Technol.*, **2**, 75 (1996).
16. Audebert P. et al. *Phys. Rev. Lett.*, **73**, 1990 (1994).
17. Lysak T.M., Trofimov V.A. *Zh. Vychisl. Mat. Mat. Fiz.*, **42**, 1275 (2001).
18. Lysak T.M., Trofimov V.A. *Opt. Spektrosk.*, **93**, 709 (2002).
19. Trofimov V.A. *Opt. Eng.*, **50**, 084201 (2011).
20. Agrawal G.P. *Nonlinear Fiber Optics* (San Diego, Cal.: Elsevier, 2007).